

**Research Article****Performance analysis in a two-phase interleaved DC-DC boost converter with coupled inductors****Selami BALCI^{a*}** **and Kadir SABANCI^a** ^a*Karamanoglu Mehmetbey University, Faculty of Engineering, Department of Electrical and Electronics Engineering, Yunus Emre Yerleskesi, 70200, Karaman, Turkiye.*

ARTICLE INFO

Article history:

Received 28 October 2022

Accepted 26 December 2022

*Keywords:*coupled inductor
boost converter
power electronics
voltage ripple
FEA

ABSTRACT

In this study, the inductor current ripple and output voltage ripple of a two-phase DC-DC boost converter, circuit performance is investigated according to the direct/inverse coupling effect of the coupled inductors. The coupled inductors are modeled with both power electronics circuit and electromagnetic modeling and by using finite element analysis software (FEA). However, the high frequency inductor designs generally use air-gapped composite ceramic ferrite cores and are designed with powder core (Kool Mu) core structures that eliminate air gap requirements. Thus, the fringe flux, which occurs in the air gaps in ferrite cores and reduces the useful flux, and the bad effects such as overheating and electromagnetic noises (EMI/EMC) in the air gaps in high frequency switching are also reduced. Especially in interleaved power converter designs, the performances of coupled inductors affect the output parameters of the power electronics circuit. Considering energy efficiency and more compact circuit topologies, the modeling and simulation approach of high-frequency inductors using finite element analysis software, which is emphasized in this study, popularly and scientifically guides power electronics circuit designers.

This is an open access article under the CC BY-SA 4.0 license.
(<https://creativecommons.org/licenses/by-sa/4.0/>)

1. Introduction

DC-DC power converter circuits are widely used in power electronics and industrial electronics applications such as electric vehicles, uninterruptible power supplies (UPS), DC power transmission-distribution systems and renewable energy sources. They perform the functions of adapting (increasing and/or decreasing) the DC voltage level required by the application areas to the desired values. Today, the application areas of DC-DC power converter circuits are quite wide as an integral element of electric power systems with various topologies in many technologies such as power electronic interfaces and electric vehicle / charging station power systems used in grid integration with renewable energy sources. As it is known, DC-DC power converter circuits are circuit topologies consisting of a semiconductor switch and passive circuit elements, and they increase or decrease the DC voltage level. In the power conversion here, the

integration of electromagnetic design information for the design of magnetic circuit elements such as inductor/transformer, as well as power electronics circuit theory and application information, plays an active role in improving its performance.

In the design of magnetic circuit elements, based on the efficiency of the system in the power electronics circuit, the saturation of the cores and the temperature increase accordingly are of great importance in terms of performance. In addition, geometric shapes in different structures and sizes such as EE, EI, toroid, pot and block can be used in the core parts [1]. Generally, composite ceramic core materials such as Ferrite and Kool-Mu are preferred for high frequency applications produced by manufacturers in standard sizes. In the design of the power electronics circuit, standard size cores can be combined to obtain the required volume by considering the inductor current fluctuation value for the rated power at kW levels (generally for maximum 20% fluctuation) [2].

* Corresponding author. E-mail address: snalci@kmu.edu.tr
DOI: 10.18100/ijamec.1195840

Silicon-based MOSFETs, which are among the power switches frequently used in practice, become conductive when used at high power, and power losses increase when they are used at higher switching frequency values than the mid-frequency values of IGBTs. Increases in power loss values limit the use of power electronics circuit structures at much higher powers and do not allow more compact topologies. On the other hand, not only the behavior of the switching elements affects the efficiency of a power electronics circuit and the volumetric power density in kW/m³. Magnetic circuit elements such as inductors and transformers must be resistant to high frequency switching. The effects of magnetic materials used in core structures of inductors and transformers on sizing and power losses are enormous [3]. In addition, core materials used for air-gapped designs in inductors core structures and special composites with air-gapped properties have also been commercially presented.

When the literature is scanned, studies with similar diversity can be seen such as coupled and uncoupled DC-DC converters, coupled reducing converters, and coupled in-line structures, inductor designs for high-frequency converters, comparison of insulated and non-insulated DC-DC converters. In a study aimed at the design of high-frequency magnetic circuit elements, it was reported that as the frequency value increases, amorphous materials give better results, but there are limitations in very high frequency values due to the difference in application ranges. It has been explained that optimum results in different frequency values, operating temperatures and applications will be achieved with high-frequency magnetic materials such as ferrite and nanocrystal. It has been reported that in a power electronics application where both volume and weight are important in inductor and transformer design, size reduction can be reduced with higher frequency. In addition, it has been concluded that if the operating frequency value is not increased, the reduction in weight and volume can only be achieved by choosing a more specific core material, which will increase the cost [4].

In a study on the applications of multi-phase coupled inductor DC-DC power converters in electric vehicles, an inductor set coupled to a four-phase 14V-42V power converter was designed. In addition, the combined common core inductor structure is also optimized. In the process of determining the superior properties of coupled inductors, simulation and experimental studies were examined in detail. [5]. In a thesis study on multi-phase DC-DC converters, detailed analyzes were made to investigate the direct benefits of coupled inductors. It has been concluded and confirmed by simulation studies that multi-phase DC-DC power converters are generally effective in current fluctuations, ripples are reduced

compared to uncoupled inductors, and coupled inductors have various electromagnetic advantages such as low sensitivity to input changes at high frequencies [6].

In a doctoral thesis investigating the effects of load changes on the output of power converters, multi-phase coupled inductor attenuation converters were examined and performance improvements were made [7]. In the master's thesis on the design of coupled inductor dc (reducing-boosting) power converters operating in continuous transmission mode, firstly, the coupled inductors and common core inductor structures used in cuk converter topologies were analyzed. Thus, the benefits and design constraints of using coupling magnetic circuit elements are presented. The selection of magnetic circuit elements such as inductors and the importance of coupled inductors providing a ripple-free input current waveform in providing continuous conduction mode are explained [8].

Phase shift technique was applied in the master's thesis in which a DC-DC reducing power converter circuit that can operate at lower switching frequencies depending on the number of phases was experimentally realized. For this purpose, the sequential reducing converter, which can operate in parallel with an appropriate number of parallels according to the current requirement, which quadruples the total switching frequency effect, was first simulated in the MATLAB/Simulink environment and experimental studies were carried out with the 16-bit dsPIC30F2020 processor used as the controller. Thus, the results obtained from the simulation and application are presented with the advantages of the sequential attenuating converter structure over the classical attenuating converter structure [9]. In a doctoral thesis in which coupled inductors are used and multi-input DC-DC topologies are proposed, high voltage gains can be obtained thanks to coupled inductances. Leakage inductances do not cause any stress on switches and diodes, while isolation is provided between the input and output of the DC-DC converter. Thus, in simulation and experimental studies, over 90% efficiency was obtained at 300 W output power from 25V input voltage to 400 V output voltage [10]. In an article on the analysis and design of coupled inductors for two-phase in-line DC-DC power converters, the effect of the coupled design on the inductor and output current ripple is examined in detail. As a result of the analysis, it was also determined that the coupling coefficient should be high enough to effectively reduce the inductor current ripple [11].

In a study designed for a target application where very high voltage gain is required, it is suggested that the voltage gain value can be made by changing the duty cycle or by changing the conversion ratio between the inductor windings. For this purpose, the 1 kW prototype power

converter was designed to test the theoretical analysis. The results show that the proposed converter achieves very high voltage gain, while the highest efficiency exceeds 96% even when two additional diodes and an additional winding are applied to the main circuit of the converter for the designed prototype. Therefore, the presented converter can be a suitable solution for applications where DC bus voltage with very low ripple is required [12].

In this study, the designs of high frequency inductors in DC-DC boosting power converter circuits, which are frequently used in power electronics applications were carried out using FEA software. In the design of power electronics circuits, the performances of magnetic circuit elements such as inductors and transformers interact with each other and optimization processes for the control of semiconductor power switches are not sufficient. For this purpose, the effects of the behavior of inductors on the ripple value of the output voltage in power electronics circuits were investigated together with the direct and inverse coupling effects.

2. Materials and Method

In this section, different core materials and structures used in high frequency inductor design are introduced. Electromagnetic performances of coupled and uncoupled inductors modeled and simulated with finite element analysis (FEA) software are emphasized.

2.1. Inductor core structures

It is essential to obtain the desired inductance value for the design of the inductor, and besides the mechanical properties such as the core cross-section and window area to be used for this purpose, the magnetization behavior of the core material (BH curves), the number of turns, roll-off values, loss and affects the technical features such as temperature rise values. In this context, the saturation flux values of ferrite materials are approximately 0.36 T, and air gaps are placed between the core parts in order to offset the magnetic saturation value in ferrite core inductors. Although the estimation of the air gap distance can be calculated theoretically, in practice, as seen in Figure 1(a), negative results such as not providing the desired inductance values with the fringe flux effect, excessive temperature and vibration effects in the air gap parts may occur.

On the other hand, when Kool Mu core materials with a distributed air gap feature are used as seen in Figure 1(b), there is no need for a process such as determining the air gap distance. Also, the saturation flux of Kool Mu core materials is 1.05 T and the B-H curve is almost linear with respect to ferrite materials. In addition, there are no adverse conditions such as fringe flux, which are known as disadvantages in air gap ferrite cores, and the specific core loss values of Kool Mu core materials are also lower.

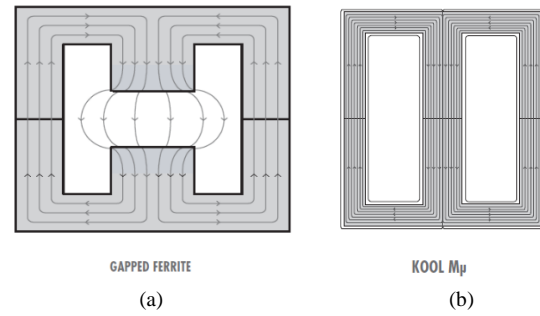


Figure 1. Flux distributions of the core structures, (a) air-gapped ferrite core, (b) powder core (Kool Mu) [13].

2.2. Electromagnetic modelling with FEA software

Electromagnetism equations are the basis of the work of electrical machines. Scottish physicist James Clerk Maxwell published these equations in 1861-1862, and Co. on electromagnetic field theory. Equations 1-4 are Maxwell's equations based on Gauss's, Faraday and Ampere's laws. Software developed for finite element analysis (such as Ansys-Maxwell, Comsol, Jmag) basically calculate based on these equations according to solvent types such as magnetostatic, electrical, electrostatic and electromagnetic transient analysis [14]. In addition, the performances of power switching elements and DC-DC converter circuits can be examined with power electronics circuit software [15, 16].

$$\vec{\nabla} \cdot \vec{E} = \frac{\rho}{\epsilon_0} \quad (1)$$

$$\vec{\nabla} \cdot \vec{B} = 0 \quad (2)$$

$$\vec{\nabla} \times \vec{E} = -\frac{\partial \vec{B}}{\partial t} \quad (3)$$

$$\vec{\nabla} \times \vec{B} = \mu_0 \vec{J} + \mu_0 \epsilon_0 \frac{\partial \vec{E}}{\partial t} \quad (4)$$

In these equations, magnetic flux density (B) in Tesla, electric field (E) in Volts/cm, current density (J) in A/mm², conductivity in siemens (ρ), permeability of space in 4·π·10⁻⁷ H/m (μ₀) and finally 8.854 pF/m is expressed as the insulation coefficient of the cavity (ε₀) [15].

The simple steps followed to design and simulate electrical machines such as transformers, electric motors and generators with finite element software is the basic flow diagram for electromagnetic modeling shown in Figure 2. According to the steps in this flow diagram, electromagnetic behavior and power losses of magnetic circuit elements such as inductors and transformers can be determined. In addition, power losses in the core structures can be estimated by parametric analysis depending on the switching frequency [17].

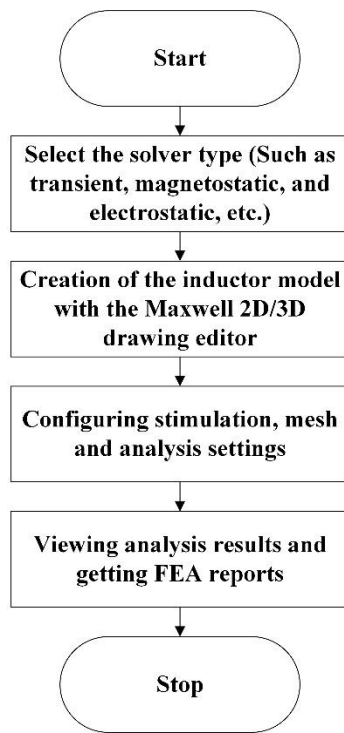


Figure 2. Basic flowchart for electromagnetic modeling [14].

2.3. Designing of the inductors

Simulation studies were carried out with electromagnetic 3D modeling using ANSYS Electronics Desktop 2019R3 academic version FEA software. In line with the results obtained from these studies, distributed air gap Kool Mu inductors were designed for the 500 uH inductance value given in Figure 3.

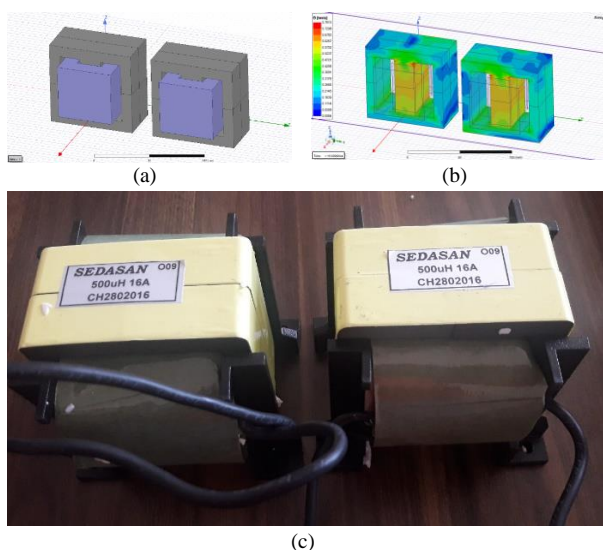


Figure 3. 500 uH uncoupled inductors with KoolMu core, (a) Modeling 3D image, (b) electromagnetic behavior simulation image (c) prototype image of inductors

For the use of these inductors with loose coupling in the common core structure, the inductors for the design and subsequent 2x500 uH inductance values are shown in

Figure 4. Here, both inductor windings are placed on the outer legs of the coupled inductors obtained with the block Kool Mu cores for loosely coupling ($k < 0.5$). In this design, since the flux circulating in the core and the total flux passing through the middle leg change depending on the direction of current passing through the windings, the power electronics circuit performance differs with the effects of direct and inverse coupling [18].

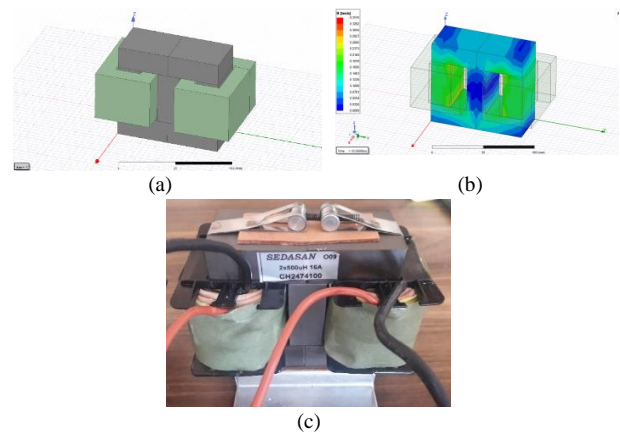


Figure 4. Kool Mu core coupled inductors, (a) Modeling 3D image, (b) electromagnetic behavior simulation image, (c) image of loosely coupled inductors (2x500 uH).

2.4. Simulation studies

An example power electronics circuit for a two-phase cascade boosting power converter is shown in Figure 5. The materials required for the construction of this power electronic circuit are given in Table 1.

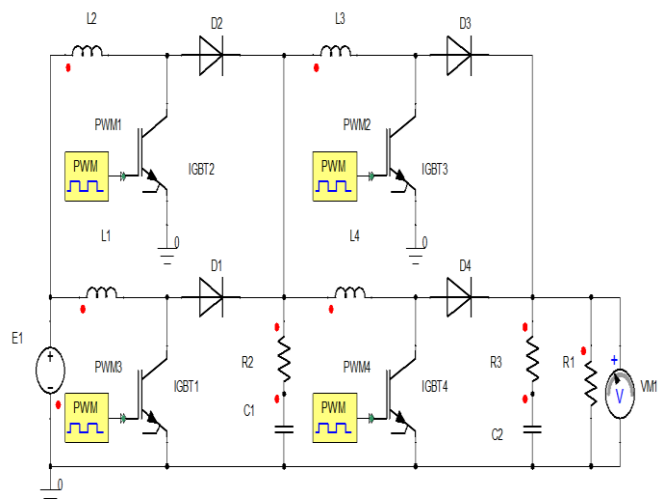


Figure 5. Two-phase interleaved cascade boost converter topology.

The current drawn from the DC source at the input of this power electronics circuit is the sum of the current of the L1, L2, L3 and L4 inductors as shown in Figure 6. Thus,

the advantage of using an inductor coupled with the proposed sequential power converter topology within the scope of simulation studies is clearly seen.

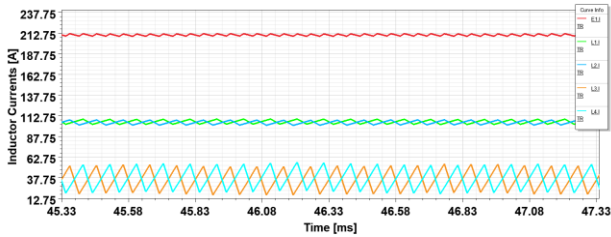


Figure 6. Current waveform drawn from the source at the input of the power converter circuit

As a result, the waveform of the output voltage of the designed two-phase cascade interleaved boosting converter circuit is shown in Figure 7. Thus, the 48 V DC input voltage is increased to approximately 380 V at the output of the power converter circuit.

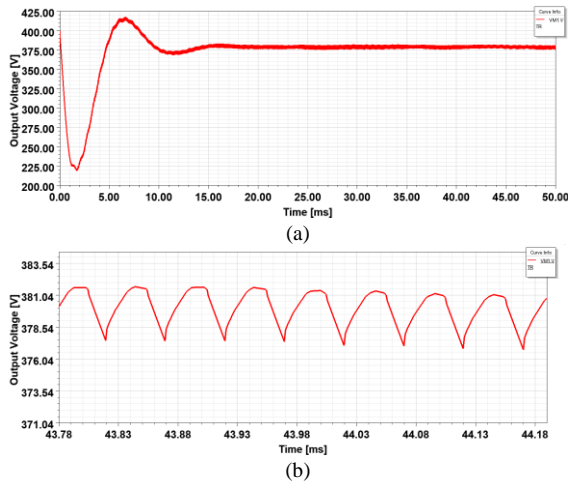


Figure 7. The output voltage of the power converter circuit, (a) voltage waveform, (b) ripple density.

Electromagnetic behavior and power electronics circuit performance in coupled inductor design differ compared to uncoupled split-core inductor structures. In particular, the differences in flux distributions of the inductor core depending on whether it is direct or inverse coupling can be easily understood from the results obtained from the electromagnetic modeling software seen in Figure 8 and Figure 9.

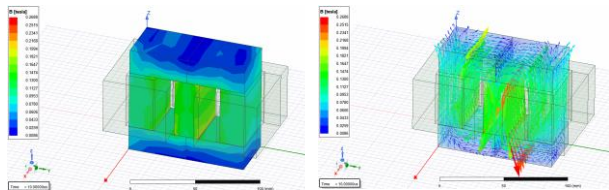


Figure 8. Flux distributions in direct coupled inductors.

In the direct-coupled case, the flux directions of the coils on the outer legs support each other and the magnetic flux passing in the same direction in the middle leg of the core is added to each other.

Here, since both windings are on the outer legs, the coupling coefficient is set to 0.20 and is called loosely coupling. In direct-coupled connection, since the flux value in the middle leg of the core is higher than the outer legs, the performance of the DC-DC power converter circuit is affected since the inductance values of the windings in the outer legs are smaller than in the inverse-coupled design.

In the inverse-coupled case, as can be seen in Figure 9, flux transitions in the middle leg of the core are opposite to each other and weaken each other in the middle leg, according to the current directions passing through the windings. However, the flux value in the outer legs of the inductor core is higher than in the inverse-coupled design due to the encounter in flux transitions in the middle leg section. However, as tightly coupling, inverse coupling is recommended for DC-DC circuits, and for loosely coupling, inverse coupling gives good results in terms of efficiency.

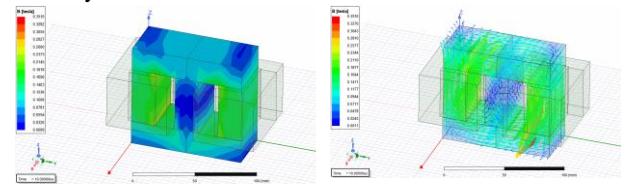


Figure 9. Flux distributions in inverse coupled inductors.

2.5. Experimental studies

The effects of the coupled and uncoupled inductors in the two-phase interleaved DC-DC boost converter circuit experiment setup with an input voltage of approximately 50 V were examined with output voltage graphs. Using the supplied consumables and the camel elements in the list given in Table 1, a two-phase interleaved DA-DA boost power converter circuit was installed and the performance analyzes of the inductors were carried out experimentally.

Table 1. Power electronics circuit materials

Sequence No.	Circuit materials
1	450 V 470 uF capacitors
2	20 cm block heatsinks
3	75 A, 600 V Half Bridge IGBT modules
4	Isolated Dual IGBT Drivers

Two-phase switching signals produced with 180° phase difference are given in Figure 10. These switching signals are connected to the IGBT1 and IGBT2 pins of the driver boards. Thus, PWM switching signals can be produced as +15 and -8 V in two phase isolation. Here, bringing the signal to -8 V levels is very important for effective transmission/turn-off modes so that the power switches can be turned off effectively. According to the waveforms of the switching signals obtained on the oscilloscope, approximately 4 μs of dead time is left between both signals and IGBTs are driven by these signals.

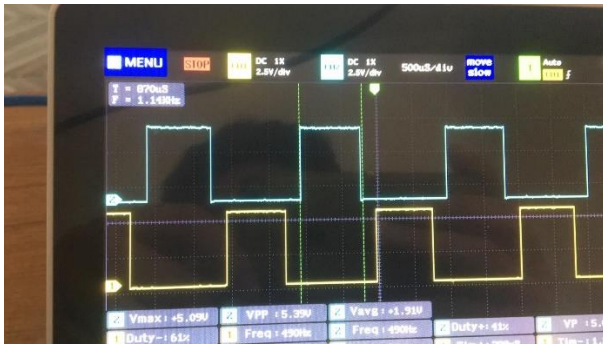


Figure 10. Two-phase switching signals with 180° phase difference.

The experimental circuit view of the use of two uncoupled inductors in the interleaved DC-DA boost power converter circuit designed as two-phase is given in Figure 11. In this circuit, the DC input voltage at the level of about 50 V was increased to 151 V while the switching duty ratio was 0.65 at the output of the converter circuit.

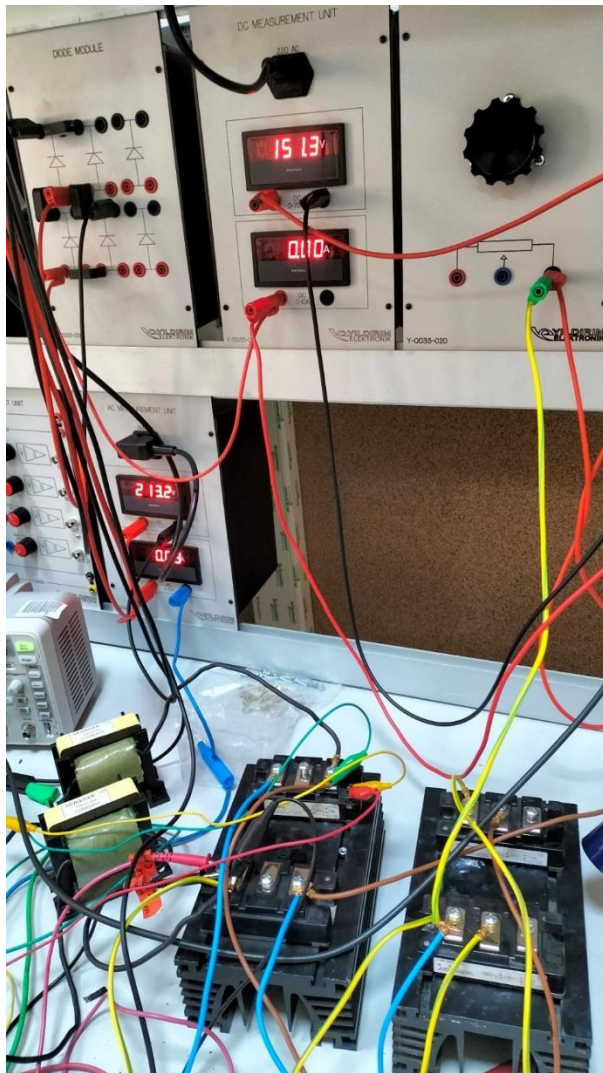


Figure 11. Two-phase interleaved DC-DC boost converter circuit with uncoupled inductors.

Here, the power switches are driven with a symmetrical two-phase PWM signal with a switching frequency of approximately 5 kHz. In this case, the oscilloscope screenshot showing the fluctuation of the output voltage is shown in Figure 12.

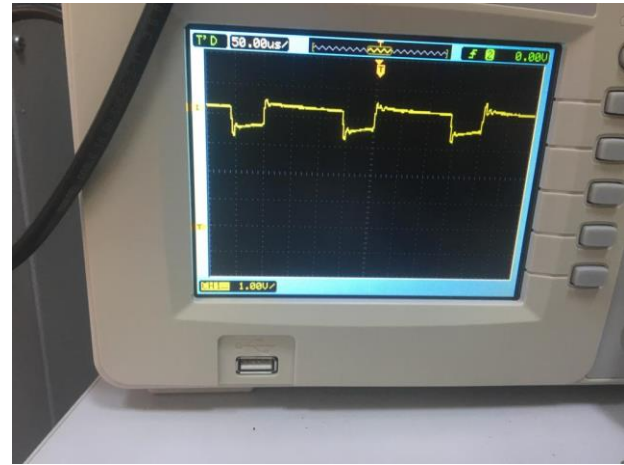


Figure 12. Output voltage waveform of two-phase interleaved DC-DC boost converter circuit with uncoupled inductors.

In the same power electronics circuit, the uncoupled inductors were deactivated and replaced with the coupled inductors shown in Figure 13. In this case, a decrease in the ripple value of the output voltage was observed under the same switching frequency and duty ratio conditions with the coupling effect.

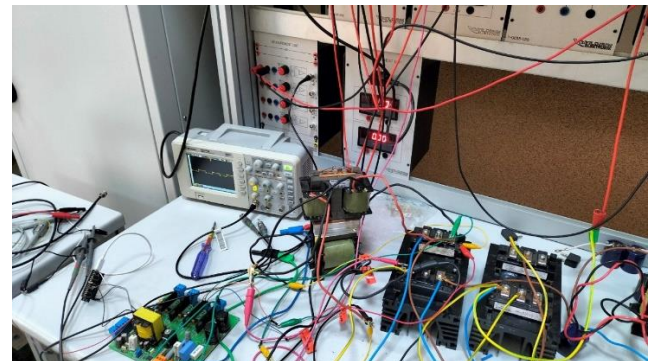


Figure 13. Two-phase interleaved DC-DC boost converter circuit with coupled inductors (direct coupling connection).

First the direct coupling connection was tested and smaller amplitude ripple was obtained according to the design of uncoupled inductors according to the DC output voltage waveform given in Figure 14.

As can be seen clearly from the DC output waveform given in Figure 15, when the connection is made in order to see the inverse coupling effect in the design where the coupled inductors are connected, the current directions through the inductors will be opposite to each other, and less fluctuation occurs. Thus, it has been revealed that a more uniform DC voltage is obtained at the output voltage with the inverse coupling effect in the coupled inductor design.

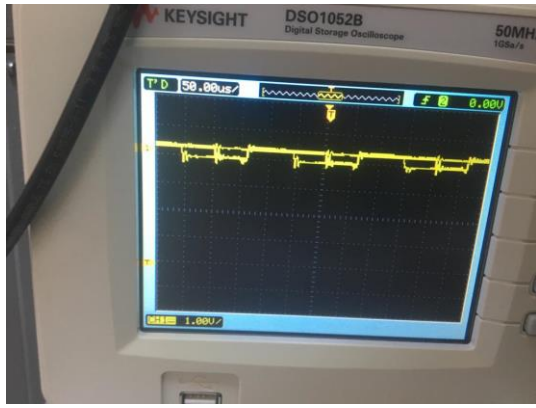


Figure 14. Output voltage waveform of two-phase interleaved DC-DC boost converter circuit with coupled inductors (direct coupling connection).



Figure 15. Output voltage waveform of two-phase interleaved DC-DC boost converter circuit with coupled inductors (inverse coupling connection).

3. Conclusions

In this study, the proposed approach regarding the design of coupled inductors and their use in DC-DC power converter circuits has been supported by simulation and experimental studies. As a result of the experimental studies, it has been determined that the two-phase interleaved DC-DC boost power converter circuit of the coupled inductor design reduces the ripple rate of the output voltage on the load and reduces the filter requirements. In addition, the differences between direct and inverse coupling connections were also analyzed by simulation and experimental studies. It has been reported that the output voltage fluctuation in inverse coupled design is smaller than in direct coupled design, the most important reason for this is that the electromagnetic flux behavior of the core outer legs varies considerably compared to the direct coupled design.

As a result, it has been an original academic study with simulation and experimental studies on the design and simulation of inductors with electromagnetic modeling software for DC-DC power converters. Especially, the

design of magnetic circuit elements such as inductors, which is one of the main objectives of this study, can be done more effectively with FEA software, and it positively affects the process of determining the effects of the effects of the power electronic circuit on the behavior of the power electronic circuit with simulation studies before the prototype production of the designed inductors thanks to electromagnetic modeling. In this context, performance in a power electronics circuit does not only depend on the control strategy of the power switches. Electromagnetic performance of inductors and different design styles and design knowledge of magnetic circuit elements also affect the efficiency and performance of power electronic circuits. As future studies, the thermal behavior of coupled inductors can be examined and their use and performance in different power electronic circuits can be examined.

Different power electronics circuits can be built using modern switching elements such as SiC or GaN for performance analysis of the coupled inductors discussed in this study for future experimental studies in higher power and higher frequency applications.

Acknowledgment

This research was supported within the scope of the project numbered 09-M-19, which was accepted by the Scientific Research Projects Commission of Karamanoglu Mehmetbey University.

References

- [1] S. Balci, "DA-DA Dönüştürücü Devreleri için Çeşitli İndüktör Nüve Şekillerinin Elektromanyetik ve Mekanik Etkileri Üzerine Karşılaştırmalı Bir Benzetim", *Düzce Üniversitesi Bilim ve Teknoloji Dergisi*, vol. 7, no. 3, pp. 1130-1139, Jul. 2019.
- [2] P. Arıkan, S. Balci and F. Battal, "Determination of the roll-off value in the air-gapped inductor of a DC-DC boost converter circuit with FEA parametric simulations", *Balkan Journal of Electrical and Computer Engineering*, vol. 8, no. 2, pp. 135-141, Apr. 2020.
- [3] S. Balci, "The Co-Simulation Studies of the Power Electronic Circuits with FEA Software". *9th Eur. Conf. Ren. Energy Sys.* 21-23 April 2021 Istanbul, Turkey.
- [4] A. A. Yarış, "Yüksek Frekanslı Güç Çeviricilerinde Transformator ve İndüktör Tasarımı", *Yüksek Lisans Tezi*, İstanbul Teknik Üniversitesi, Fen Bilimleri Enstitüsü, İstanbul, 2001.
- [5] J. Czogalla, Jieli Li and C. R. Sullivan, "Automotive application of multi-phase coupled-inductor DC-DC converter", *38th IAS Annual Meeting on Conference Record of the Industry Applications Conference*, Vol. 3, pp. 1524-1529, 2003.
- [6] M. Shi, "Design and analysis of multiphase DA-DA converters with coupled inductors", *MSc Thesis*, Texas A&M University, Texas A&M University, 2007.
- [7] Y. Dong, "Investigation of Multiphase Coupled-Inductor Buck Converters in Point-of-Load Applications", *Doctoral Thesis*, Virginia Polytechnic Institute and State University, 2009.
- [8] M. T. Ayhan, "Design and Implementation of Coupled Inductor Cuk Converter Operating in Continuous Conduction Mode", *MSc thesis*, The Graduate School Of Natural Aand Applied Sciences Of Middle East Technical University, 2011.
- [9] I. Sefa, F. Battal and S. Balci, "Modeling and implementation of dsPIC based interleaved buck converter," 4th International

- Conference on Power Engineering, Energy and Electrical Drives, 2013, pp. 1652-1657, doi: 10.1109/PowerEng.2013.6635865.
- [10] F. Evran, "Yüksek Gerilim Kazançlı Kuplajlı Endüktör Kullanılan Z-Girişli DA-DA Dönüştürücü Topolojileri", *Doktora Tezi*, Gazi Üniversitesi, Fen Bilimleri Enstitüsü, Ankara, 2012.
- [11] J. Lee, H. Cha, D. Shin, K. Lee, D. Yoo and J. Yoo, "Analysis and Design of Coupled Inductors for Two-Phase Interleaved DC-DC Converters," *Journal of Power Electronics*, vol. 13, no. 3, pp. 339-348, 2013.
- [12] M. Frivaldsky, B. Hanko, M. Prazenica, J. Morgos. "High Gain Boost Interleaved Converters with Coupled Inductors and with Demagnetizing Circuits", *Energies*, 11(1):130, 2018.
- [13] Magnetics Powder Core Material KoolMu26u datasheet, Erişim: <https://www.mag-inc.com/Media/Magnetics/Datasheets/0078074A7.pdf>, 2018, 31 December.
- [14] B. Aslan and S. Balci , "Sonlu Elemanlar Analizi Yazılımı ile IPM Mil Motor Performans Analizi Üzerine Karşılaştırmalı Bir Benzetim Çalışması", *Muş Alparslan Üniversitesi Mühendislik Mimarlık Fakültesi Dergisi*, vol. 2, no. 2, pp. 81-90, Dec. 2021.
- [15] J.P.A. Bastos and N. Sadowski, "Electromagnetic Modeling by Finite Element Methods", Universidade Federal de Santa Catarina Florianopolis, Brazil, Copyright by Marcel Dekker. 2003.
- [16] Sabancı K. , Balci S. , Aslan M. F. Estimation of the switching losses in DC-DC boost converters by various machine learning methods. *Journal of Energy Systems*. 2020; 4(1): 1-11.
- [17] B. Aslan, S. Balci, A. Kayabasi, and B. Yildiz., "The core loss estimation of a single phase inverter transformer by using adaptive neuro-fuzzy inference system", *Measurement*, Volume 179, 2021, 109427.
- [18] S. Balci, N. Altin, H. Komurcugil and I. Sefa, "Performance analysis of interleaved quadratic boost converter with coupled inductor for fuel cell applications," *IECON 2016 - 42nd Annual Conference of the IEEE Industrial Electronics Society*, 2016, pp. 3541-3546, doi: 10.1109/IECON.2016.7794045.